TECHNICAL REPORT

ISO/TR 17321-5

First edition
2021-01

Graphic technology and photography — Colour characterization of digital still cameras (DSCs) —

Part 5: Colour targets including saturated colours for colour characteristic evaluation test for colorimetric image capture

Technologie graphique et photographie — Caractérisation de la couleur des appareils photonumériques —

Partie 5: Cibles de couleurs incluant des couleurs saturées pour l'essai d'évaluation des caractéristiques chromatiques pour la capture d'images en mode colorimétrique

Reference number
ISO/TR 17321-5:2021(E)

ISO copyright office
CP 401 • Ch. de Blandonnet 8
CH-1214 Vernier, Geneva
Phone: +41 22 749 01 11
Email: copyright@iso.org
Website: www.iso.org

Published in Switzerland

Contents

Page

Foreword

ISO (the International Organization for Standardization) is a worldwide federation of national standards bodies (ISO member bodies). The work of preparing International Standards is normally carried out through ISO technical committees. Each member body interested in a subject for which a technical committee has been established has the right to be represented on that committee. International organizations, governmental and non-governmental, in liaison with ISO, also take part in the work. ISO collaborates closely with the International Electrotechnical Commission (IEC) on all matters of electrotechnical standardization.

The procedures used to develop this document and those intended for its further maintenance are described in the ISO/IEC Directives, Part 1. In particular the different approval criteria needed for the different types of ISO documents should be noted. This document was drafted in accordance with the editorial rules of the ISO/IEC Directives, Part 2 (see www.iso.org/directives).

Attention is drawn to the possibility that some of the elements of this document may be the subject of patent rights. ISO shall not be held responsible for identifying any or all such patent rights. Details of any patent rights identified during the development of the document will be in the Introduction and/or on the ISO list of patent declarations received (see www.iso.org/patents).

Any trade name used in this document is information given for the convenience of users and does not constitute an endorsement.

For an explanation of the voluntary nature of standards, the meaning of ISO specific terms and expressions related to conformity assessment, as well as information about ISO's adherence to the World Trade Organization (WTO) principles in the Technical Barriers to Trade (TBT), see www.iso.org/iso/foreword.html.

This document was prepared by Technical Committee ISO/TC 42, *Photography*.

A list of all parts in the ISO 17321 series can be found on the ISO website.

Introduction

There are many application areas such as medical imaging, cosmetics, e-commerce, sales catalogue, fine art reproduction, art archive etc. where colorimetric image capture and colorimetric image reproduction are desired. When precise colorimetric reproduction is required for the subjects that include highly-saturated colours, it is desirable that overall sensor spectral sensitivities are close to linear combinations of CIE 1931 colour matching functions.

On the other hand, real DSCs have overall sensor spectral sensitivities that deviates from linear combination of CIE 1931 colour matching functions, and yet reproduces reasonable colours for general low-saturated colour objects. This is because most of spectral distribution of real-existing objects are well self-correlated in the wavelength direction. This is also true for the frequently-used colour target such as X-rite colour checker classic.

Therefore, when the precise colour reproduction is required for highly-saturated colour objects, it is important to use spectral distribution that are less self-correlated in the wavelength direction, for the evaluation of overall sensor spectral sensitivities.

For this purpose, Clause 3 proposes two methods for generating highly-saturated colour targets. The first method is statistical extension of existing objects spectra, and the second one is selection from artificial (LED-based) spectra.

Clause 4 then describes how these highly-saturated colour targets can be used for goodness evaluation of overall sensor spectral sensitivities. Applicability of several existing evaluation metrics (such as Vora's μ-factor and Sharma's FOM) are compared, using highly-saturated targets generated by the methods proposed in Clause 4.

Annex B gives details on colour gamut of boundary colour and Annex F gives more information on colour differences of patches of CDSW target.

Graphic technology and photography — Colour characterization of digital still cameras (DSCs) —

Part 5:
Colour targets including saturated colours for colour characteristic evaluation test for colorimetric image capture

1 Scope

This document describes sample methods to generate spectra for colour targets comprised of highly saturated colours for colour characteristic evaluation of colorimetric image capture capability of digital still cameras (DSCs).

2 Normative references

There are no normative references in this document.

3 Terms and definitions

For the purposes of this document, the following terms and definitions apply.

ISO and IEC maintain terminological databases for use in standardization at the following addresses:

— ISO Online browsing platform: available at https://www.iso.org/obp

— IEC Electropedia: available at http://www.electropedia.org/

3.1
colour-difference-sensitive wavelength
CDSW
wavelength sensitive to colour difference

3.2
colour matching functions
tristimulus values of monochromatic stimuli of equal radiant power

[SOURCE: CIE Publication 17.4, 845-03-23]

3.3
digital still camera
DSC
device which incorporates an image sensor and produces a digital signal representing a still picture

[SOURCE: ISO 12232:2012, 3.40, modified — Notes 1 and 2 to entry have been deleted.]

3.4
light-emitting diode
LED
semiconductor diode that emits non coherent optical radiation through stimulated emission resulting from the recombination of electrons and photons, when excited by an electric current

[SOURCE: IEC 60050-521, 521-04-39]

3.5
overall sensor spectral sensitivities
OSSS
spectral sensitivities of overall sensor components, which could be derived as spectral sensitivities' product of optical elements (including IR/UV-cut filter), colour filter sets, and image sensor

3.6
tristimulus values
amounts of the three reference colour stimuli, in a given trichromatic system, required to match the colour of the stimulus considered. *(see colour matching functions)*

[SOURCE: CIE Publication 17.4, 845-03-22]

4 Highly-saturated colour targets

4.1 General

This document proposes two different methods for generating highly-saturated colour targets.

First one is "Extension of real existing spectra using an eigenvector method". Naturally existing saturated colour spectra are usually very difficult to obtain by measurement. Therefore, computed spectra are extended from the eigenvectors generated from spectral databases.

Second one is "Artificial (LED-based) spectra whose wavelength peak is on colour-difference-sensitive wavelength (CDSW)". Mathematical analysis was performed to select the wavelengths which were colour-difference-sensitive. Artificial (LED-based) spectra were then generated whose peak matches colour-difference-sensitive wavelength (CDSW).

4.2 Extension of real existing spectra using eigenvector method

4.2.1 General

The eigenvector-based procedure for generating highly-saturated colour targets is as follows:

— selection of spectral database (see 4.2.2);

— spectral reconstruction from the eigenvectors (see 4.2.3);

— calculation of boundary colours (see 4.2.3.2);

— calculation of saturated-colours using reference spectral distribution (see 4.2.3.3).

4.2.2 Selection of spectra database

The wavelength range and wavelength increment are user-definable. ISO 17321-1[7] described that the wavelength range is 380 nm to 730 nm with a sampling interval of 10 nm or less. The spectral distribution set selected depends on user's application.

The brightness level of the spectral distribution selected can be ignored because the brightness level is tuneable by scaling the eigenvectors used for spectral distribution reconstruction. Hue angle of the selected spectral distribution is very important and the use of evenly-spaced hue angle is recommended.

An example of the eigenvector sets (E_{ij}) is calculated on the selected spectral distribution set (described in Annex A).

4.2.3 Spectral reconstruction from the eigenvectors

4.2.3.1 General

Spectra from the original dataset using Formula 1 can be computed as linear combination of eigenvectors.

The following notation is used for this example:

M : number of wavelengths to be used,

N : number of eigenvectors to be used,

E_{ij} : i-th wavelength component of the j-th eigenvector (i = 1, M; j = 1, N),

w_j : weight of j-th eigenvector (j = 1, N),

r_i : i-th wavelength component of a spectrum (i = 1, M).

$$r_i = \sum_{j=1}^{N} \left(w_j \cdot E_{ij} \right) \tag{1}$$

Conversely, the weights required to reconstruct a reflectance spectrum from the dataset are a linear combination of the reflectance spectrum and the eigenvectors:

$$w_j = \sum_{i=1}^{M} \left(r_i \cdot E_{ij} \right) \tag{2}$$

Two cases are considered here:

a) The boundary colour case determines the set of spectra that represent the chromatic limit as a function of hue maximally achievable based on the fundamental characteristics of an underlying spectral dataset where the resulting spectra are linear combinations of a subset of selected dataset eigenvectors.

b) The saturated colour case produces arbitrary highly saturated spectra from a linear combination of a subset of selected eigenvectors of a spectral dataset even though the target spectra are not from the dataset from which the eigenvectors are computed and therefore will only be an approximate match to the target spectra.

Both use Formula (1) but have different constraint conditions for the optimization process.

4.2.3.2 Boundary colour generation

Boundary colours are those colours whose spectral distributions have maximum chroma for a given hue angle.

There are numerous ways to identify which spectral reflectance vectors r_i have to be selected. The simplest method is to index through all weights w_j at a reasonable increment to produce a large set of r_i, compute the resulting hue and chroma values for the set of r_i, then select the subset of r_i that yields maximum chroma for each hue angle of interest.

However, it is preferred to recast Formula (1) so that it can be constrained for maximum chroma, hue angle, smoothness, or other conditions that are suitable for the intended application and to use general-purpose numerical optimization methods to solve for the optimal weights w_j directly. The resulting spectral reflectance vector r_i is constrained to the range [0,0,1.0]. Annex H describes those spectral distributions.

4.2.3.3 Saturated-colour generation using the reference spectra distribution set

It is possible to approximate an arbitrary target spectrum *r* using the eigenvectors of a spectral dataset, even if the target spectrum does not share the same fundamentals as the reference spectral dataset from which the eigenvectors were derived. This approximation *r'* is the least-squares match to the target spectrum *r*, typically subject to constraints.

For instance, it is possible to calculate highly saturated colour target spectra *r'* having a C^* value larger than a reference spectrum while maintaining L^* and hue angle. This C^* for each reference colour target is determined prior to nonlinear optimization described in Annex C. Objective parameter for nonlinear optimization is to keep predetermined C^*. Annex C shows an example in the case of Pointer's surface colours. There are many metamers of the candidate spectrum and users need to select the appropriate spectrum from many metamers. This step is applicable to other cases where any reference distribution and its objective chromaticity are given.

Annex C shows a generation method which calculates spectral distribution corresponding to CIELAB values of Pointer's surface colour[6]. Annex H describes those spectral distributions.

Given an arbitrary highly saturated target spectrum *r*, the goal is to produce an approximate match *r'* from a selected subset of the eigenvectors of the reference spectral dataset. However, there are many possible candidate matches *r'* depending on the initial w_j selected for the optimization process. One approach is to compute the starting weights for nonlinear numerical optimization with Formula 2. The weights *w* are substituted into Formula 1 producing an approximate match *r'* and *w* is iterated until the error between *r'* and *r* is minimized. Using generalized numerical optimization, this method calculates w_j to minimize the sum of the squares of the differences between the closest matching spectrum achievable *r'* by the selected eigenvector subset.

4.3 Artificial (LED-based) spectra whose wavelength peak is on colour-difference-sensitive wavelength (CDSW)

4.3.1 General

The wavelength range for colour target spectra for camera uses is from 380 nm to 730 nm according to ISO 17321-1.

The CDSW-based procedure for generating highly-saturated colour targets is as follows:

— The method to define CDSW (See 4.3.2)

— Selection of CDSW (See 4.3.3)

4.3.2 The method to define the colour-difference-sensitive wavelength (CDSW)

Factors of colour difference, *Fac_a** and *Fac_b** are defined based on the colour matching functions as shown in Formulae (3) and (4). *Fac_a** and *Fac_b** are function of X and Z, respectively. The reasons and the processes of deriving *Fac_a** and *Fac_b** are described in Annex D.

$$Fac\_a^*(\lambda) = 500 \times \left\{ f\left(\frac{\bar{x}(\lambda)}{Xn} \right) - \frac{16}{116} \right\} \tag{3}$$

$$Fac\_b^*(\lambda) = 200 \times \left\{ f\left(\frac{\bar{z}(\lambda)}{Zn} \right) - \frac{16}{116} \right\} \tag{4}$$

where

$$f(t)=\begin{cases} t^{1/3}, & t>0,008856 \\ 7,787\times t+0,138. & t\le 0,008856 \end{cases}$$

Xn=0,9504, Zn=1,0889

$$\text{Diff } Fac\_a^*(\lambda)=\frac{Fac\_a^*(\lambda+\Delta)-Fac\_a^*(\lambda)}{\Delta} \tag{5}$$

$$\text{Diff } Fac\_b^*(\lambda)=\frac{Fac\_b^*(\lambda+\Delta)-Fac\_b^*(\lambda)}{\Delta} \tag{6}$$

Calculated values of the factors are drawn against wavelength in Figure 1. It can be said that the wavelength where the colour difference between the colour matching functions and the camera is most likely to be the maximum and peak wavelength of the slope of the waveform in Figure 1. Wavelength ranges where the Δa^* and Δb^* have peak values are very similar to those of the maximum, minimum and inflection points of the curves of the factors.

In order to find those points, the derivatives of *Fac_a** and *Fac_b** with wavelength as shown in Formulae (5) and (6) are calculated (Figure 2). Wavelengths at which large colour differences most likely appear are determined by the points where the derivative is maximum, minimum and crosses zero from plus to minus and vice versa. Wavelengths corresponding to those points are 420 nm, 440 nm, 480 nm, 500 nm, 505 nm, 510 nm, 600 nm and 650 nm. These wavelengths are listed Table 1 and also indicated in Figure 2.

NOTE The reasons why we use the wavelength where the derivative is maximum, minimum and zero are as follows. The optimization process to obtain conversion matrix from camera sensitivity to colour matching function was carried out using the least square method to minimize ΔS. In the process, each one of transformed XYZ functions is adjusted to one of the matching functions by increasing (decreasing) intensity at peak wavelength where the derivative is zero, and simultaneously decreasing (increasing) it at steep slope's wavelength where the derivative is maximum or minimum. Therefore, at wavelengths where derivative is maximum, minimum and zero, colour differences can often appear.

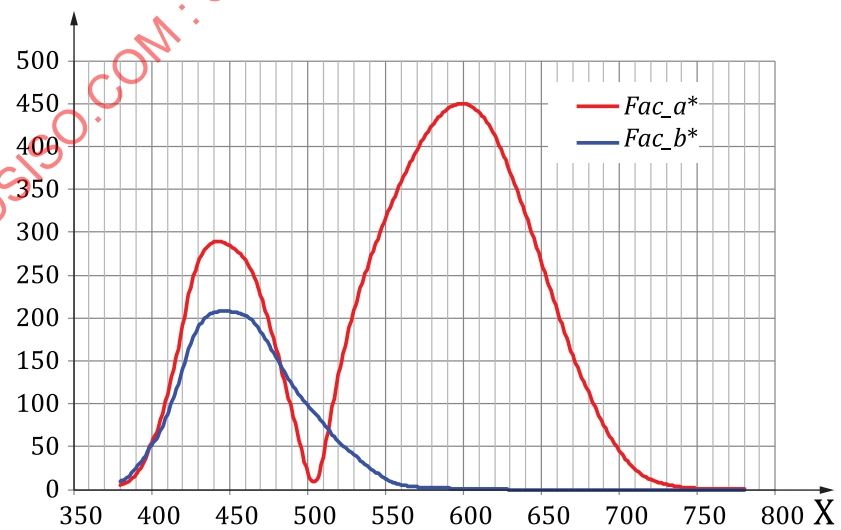

Key

X wavelength, λ, in nm

Figure 1 — *Fac_a and *Fac_b**plot against wavelength**

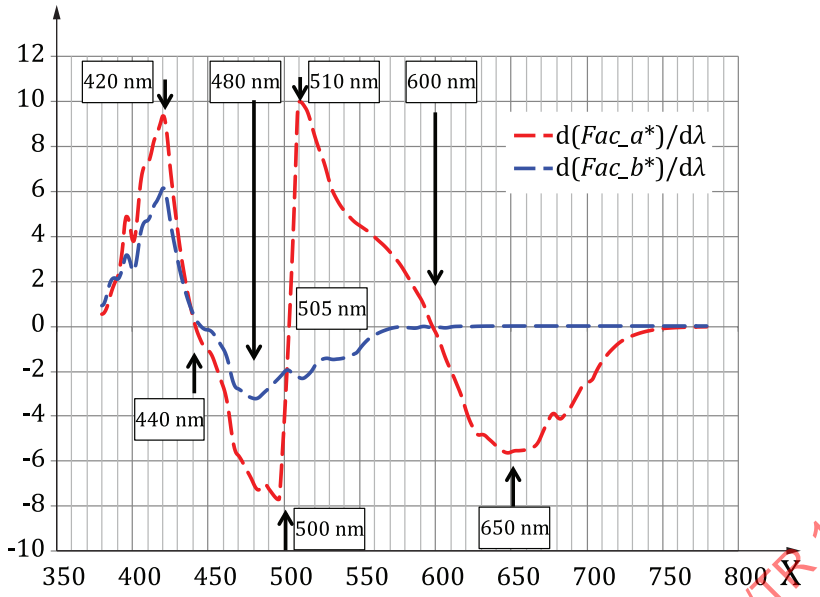

Key

X wavelength, λ, in nm

Figure 2 — Differentiated values of *Fac_a and *Fac_b***

Wavelengths of 500 nm, 505 nm and 510 nm are very close to each other and their effect on colour difference is similar and so the wavelength of 505 nm is chosen to represent these three wavelengths.

Table 1 — Candidate of CDSW corresponding to maximum, minimum and zero of derivative

	420	440	480	500	505	510	600	650
d(*Fac_a**)/dλ	max	0	min	↗	0	max	0	min
d(*Fac_b**)/dλ	max	0	↘	min	↗	↗	→	→

↗,↘ and →signs in Table 1 mean "increase", "decrease" and "no change" respectively.

Based on this analysis, wavelengths of 420 nm, 440 nm, 480 nm, 505 nm, 600 nm and 650 nm are selected as the colour-difference-sensitive wavelengths (CDSW).

4.3.3 Selection of LED for CDSW targets

In the next step, the spectral distribution of highly saturated colour target will be specified based on CDSWs.

It is ideal for CDSW target to use laser devices. However considering availability at this time, LEDs are recommended and may be more practical. Appropriate devices in accordance with technology progress in future will be adopted.

It is recommended that LEDs used for CDSW targets have the following conditions.

— Use existing LEDs which has the peak wavelength of LEDs is within +- 3 nm of CDSWs,

— Or Find similar LEDs with the peak wavelength defined by CDSW (peak does not have to be exact).

— Find LED-like width and generate the spectra artificially.

NOTE LED-like width is easily found because it is naturally determined according to LED's materials and structures at around the CDSWs.

— The shape of the spectrum is that of Gaussian distribution.

— The LEDs don't have any phosphors,

— The LEDs have no side peaks.

Figure 3 shows spectral distribution of the LEDs which are selected under above conditions.

In Figure 3, a set of realisable spectral distributions are shown corresponding to the six CDSWs.

The six-colour patches are named 'CDSW target'. Spectral values for the colours of these patches are listed in Table H.1.

For reader relevance, calculated chromaticities of the six highly saturated colours and their chromaticities as captured (and estimated) by camera A and camera B are also plotted in Figure F.1.

In addition to these CDSW targets, the colour differences are equally large for wavelengths around 410 nm on several cameras when colour difference analysis is carried out as described in Annex E. Therefore, 410 nm wavelength can be added to CDSW targets in place of 420nm wave length depending on user's application.

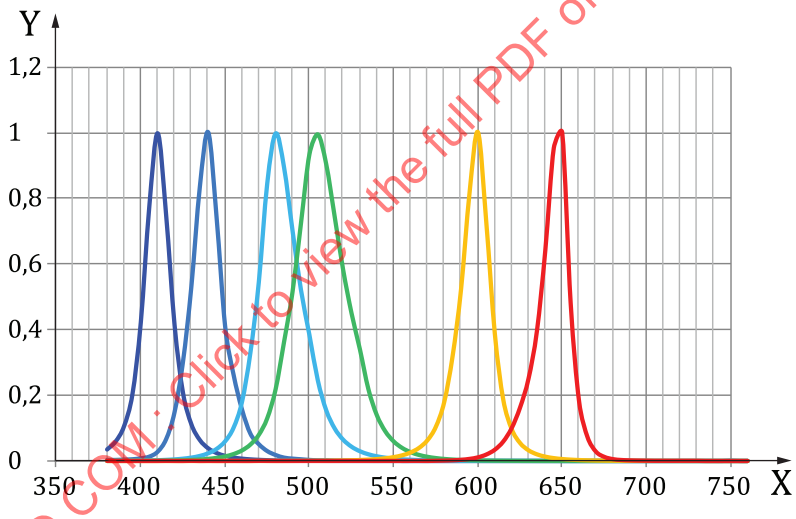

Key

X wavelength, λ, in nm

Y relative intensity

Figure 3 — Spectral distribution of each patch of CDSW target

In 2018, very wide gamut broadcast service, ITU-R BT.2020, were launched. It is very useful to show how to use CDSW targets in practice by applying to the specific system.

Annex G describes a method to define a highly saturated colour target for cameras designed to capture specific RGB colour spaces. When the destination RGB of a camera is fixed, the method for creating highly saturated colour target is explained using the ITU-R BT.2020[5] standard as an example.

5 FOM metric for evaluation of overall sensor spectral sensitivities, used in the digital cameras

5.1 General

This clause provides how the highly-saturated colour targets can be used for evaluation for overall sensor spectral sensitivities (hereafter abbreviated as OSSS), which are described in 4.2 (Extension of real existing spectra using the eigenvectors method) and 4.3 [Artificial (LED-based) spectra whose wavelength peak is on Colour-difference-sensitive wavelength (CDSW)].

5.2 Evaluation metrics for OSSS

There has been many evaluation metrics for evaluating the goodness of OSSS, such as Neugebauer's *Q*-factor[2], Vora's μ-factor[1] and Sharma's FOM.[4]. If the colour filter set is perfect linear combination of CMF (colour matching function), the value of these metrics becomes 1.00, and the value decreases as the linear combination of the OSSS deviates from CMF.

NOTE Q-factor metric evaluates sensor colour filter one by one, not as a filter set.

However, OSSS with low (i.e. bad) μ-factor could sometimes have good colour reproduction. This is because μ-factor does not consider the reflectance spectra of the target subjects at all. The distinguished difference of FOM metric to other two metrics is the consideration of reflectance spectra. Following formula indicates simplified version of FOM, and it is called FOM_S in this document. The $\boldsymbol{K_r}$ correlation matrix is used in the metric, which describes the characteristics of the reflectance spectra ***r***.

$$FOM_S\left(\boldsymbol{A},\boldsymbol{G},\boldsymbol{K_r}\right)=\frac{tr\left(\boldsymbol{A}^T\cdot\boldsymbol{K_r}\cdot\boldsymbol{G}\cdot\left(\boldsymbol{G}^T\cdot\boldsymbol{K_r}\cdot\boldsymbol{G}\right)^{-1}\cdot\boldsymbol{G}^T\cdot\boldsymbol{K_r}\cdot\boldsymbol{A}\right)}{tr\left(\boldsymbol{A}^T\cdot\boldsymbol{K_r}\cdot\boldsymbol{A}\right)} \tag{7}$$

where $\boldsymbol{K_r}=E\left\{\boldsymbol{r}\cdot\boldsymbol{r}^T\right\}=E\left\{\begin{bmatrix}\boldsymbol{r}_{1,400} & \cdots & \boldsymbol{r}_{n,400}\\ \vdots & \ddots & \vdots\\ \boldsymbol{r}_{1,700} & \cdots & \boldsymbol{r}_{n,700}\end{bmatrix}\begin{bmatrix}\boldsymbol{r}_{1,400} & \cdots & \boldsymbol{r}_{1,700}\\ \vdots & \ddots & \vdots\\ \boldsymbol{r}_{n,400} & \cdots & \boldsymbol{r}_{n,700}\end{bmatrix}\right\}$

— ***A*** is the N x 3 matrix of CIE colour matching functions (CMF).

— ***G*** is the N x 3 matrix of OSSS.

— $\boldsymbol{K_r}$ is the N x N correlation matrix defined by above formula.

— ***r*** is the reflectance spectra (400 nm to 700 nm, 10 nm interval, was used in this case).

While the original FOM paper by Sharma[4] describes many variations for the FOM metric, "Type A: XYZ mean-square-error-based FOM" was chosen for its calculation simplicity in this case. Several additional simplifications were applied to the original FOM definition. First, $\boldsymbol{K_\eta}$ term which describes measurement noise, was ignored. Since the noise is produced by the image sensor and electronic circuits, this can be considered irrelevant to the evaluation of OSSS characteristics. Second, illuminant consideration was ignored. In the Sharma's paper, since its target was colour scanners, the product of illuminant spectra and colour filter spectra was used as $\boldsymbol{A_L}$. For the digital cameras, since the illuminant cannot be predefined, the product with illuminant was not used.

When $\boldsymbol{K_r}$ becomes unity matrix $\boldsymbol{E}$, which means that there is no correlation for reflectance spectra (in the wavelength direction), $\boldsymbol{FOM_S}$ is reduced very close to the μ-factor as below, except that μ-factor uses orthonormal space for CMF (colour matching functions).

$$FOM_S\left(\boldsymbol{A},\boldsymbol{G},\boldsymbol{K_r}=E\right)=\frac{tr\left(\boldsymbol{A}^T\cdot\boldsymbol{G}\cdot\left(\boldsymbol{G}^T\cdot\boldsymbol{G}\right)^{-1}\cdot\boldsymbol{G}^T\cdot\boldsymbol{A}\right)}{tr\left(\boldsymbol{A}^T\cdot\boldsymbol{A}\right)} \tag{8}$$

Since FOM_S includes $\boldsymbol{K_r}$ term, the metric correlates well with average ΔE (deltaE) of the colour target set. This is large advantage for FOM_S over μ-factor, since the metric correlates very well with the colour reproduction, as written in the FOM paper.

5.3 Advantages and disadvantages of ΔE (delta$E$) evaluation

The average ΔE is very often used for the evaluation of colour reproduction of the digital cameras in many industrial locations. There are many advantages for using ΔE, since the final output of the camera can be evaluated. There are additional merits for ΔE, such as 1) ΔE for specific colour patch or regions could be used for comparison, 2) ΔE (delta$E$)could be broken down to specific perceptual attribute components such as ΔL, ΔC and ΔH for colour evaluations, and 3) tuning of colour conversion matrix is easily possible (e.g., putting more weights on specific colours/illuminants, and/or restricting errors on ΔL, ΔC and ΔH).

Because of this large flexibility (especially for the 3rd case), ΔE could have so many variations. In addition, CIE defines several versions for ΔE calculations; ΔE^*ab(1976), ΔE^*uv(1976), ΔE_{1994} and ΔE_{2000}. Still, improved (or upgraded) versions of ΔE (colour difference evaluation methods) are being proposed by CIE and related academic conferences. This flexibility (or variations) could often cause the big problems when making cross-comparisons, since the evaluation conditions could differ considerably from one to another. Unless these calculation conditions are rigidly controlled (i.e., every steps of the calculation with every parameters are fully documented), ΔE (delta$E$) won't be an appropriate measure for standardized cross-comparison evaluation method in industry.

NOTE For example, while $\boldsymbol{\Delta E_{2000}}$ is currently known to have the most perceptual correlation and thus recommended by CIE, the metric calculation is so complex which includes several conditional branches. Because of this high complexity, it has potential risks to fall into local minimums in optimization process and different location might obtain different results, when $\boldsymbol{\Delta E_{2000}}$ is used as error metric for (traditional) optimization calculation.

Moreover, when very saturated colours (e.g. LED colours defined in 4.3) are evaluated with real OSSS, negative XYZ values could be obtained after applying RGB-XYZ conversion. Since how to obtain CIELAB values from calculated negative XYZ values is not defined anywhere, ΔE calculations cannot be performed in these cases.

On the other hand, FOM_S's only variable is $\boldsymbol{K_r}$: correlation matrix, which describes the overall characteristics of target colour sets (to be evaluated). Once $\boldsymbol{K_r}$ is chosen, FOM_S metric will be uniquely defined at any different locations. Because of this low flexibility, FOM_S is very suitable for the cross-comparison purposes, as this method could deliver uniquely-defined standardized value.

5.4 How 17321-5 datasets can be used for *FOMs*

If the $\boldsymbol{K_r}$ is appropriately chosen, $\boldsymbol{FOM_S}$ becomes very good measure for the cross comparison for the specified colour target (or for the specified application). For $\boldsymbol{K_r}$ derivation, it is recommended to use in-site spectral radiance database (e.g. informative Annex C of ISO 17321-1) which are representative of the likely scenes or subjects to be captured, whenever possible. $\boldsymbol{K_r}$ needs to be carefully chosen for specific application, and the specifically-chosen $\boldsymbol{K_r}$ cannot be applied for different applications.

For example:

— If the colour reproduction target is less saturated colours, $\boldsymbol{K_r}$ derived from Macbeth ColorChecker (MB) could be used.

— If the colour reproduction target is highly saturated colours, K_r derived by 4.2 colour target sets (HS) could be used.

— If the colour reproduction target is extremely-saturated colours generated by artificial LED colours, K_r derived by 4.3 colour target (CDSW) sets could be used.

Following figures indicate diagonal (45°) cross-sectional view of K_r of one example of HS dataset and MB18 (first three rows of Macbeth colour checker) at 550 nm, 475 nm and 625 nm respectively. As easily seen from the figures, K_r of HS is much sharper than K_r of MB18, and is closer to the unity matrix E. This means that spectra of highly saturated colours would have lower self-correlations in the wavelength direction.

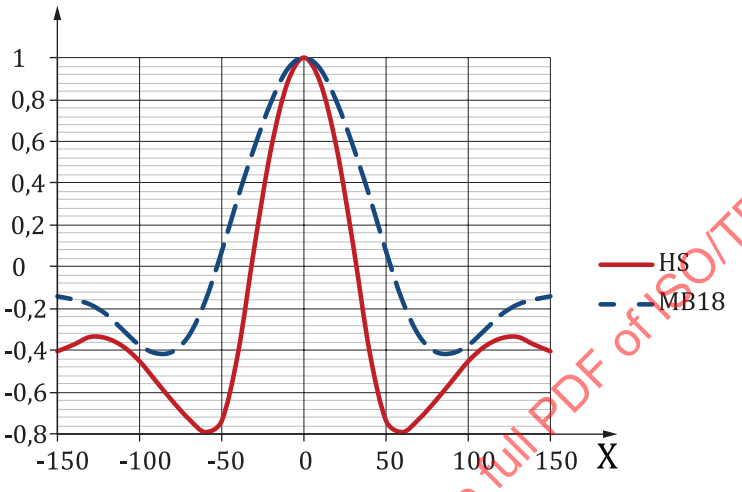

a) Kr at 555 nm

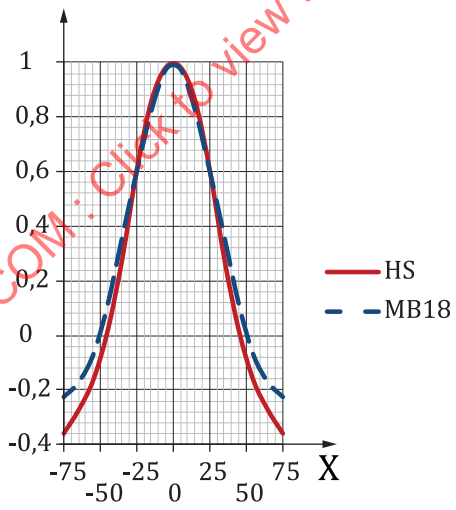

b) Kr at 475 nm

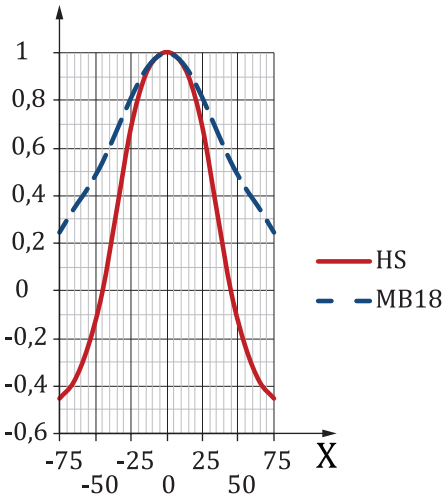

c) Kr at 625 nm

Key

X wavelength, λ, in nm

Figure 4 — Cross-sectional view of self-correlation matrix

5.5 Worked examples

Following table indicates the results of the FOM_S calculation with different K_r's for different OSSS, which are indicated in Figure 4 a), Figure 4 b) and Figure 4 c).

Table 2 — Worked example of FOM metric using different Kr's with different filter sets

Metric OSSS	μ-factor	FOM_S K_r(E)	FOM_S K_r(CDSW)	FOM_S K_r(HS)	FOM_S K_r(MB18)
OSSS A	0,9911	0,9966	0,9988	0,9999	0,9999
OSSS B	0,9225	0,9040	0,9612	0,9947	0,9971
OSSS C	0,8672	0,8516	0,9255	0,9865	0,9944

As seen from the calculated results in the Table 2, the metric difference by OSSS becomes smaller as the self-correlation matrix K_r deviates from the unity matrix E. This proves that colour reproduction with OSSS with the low (i.e. bad) μ-factor has sufficiently good result for the colour reproduction of comparatively low-saturated colour sets, such as MB18. On the other hand, it is noted that difference in μ-factor metric is excessive (or exaggerated) for colour reproduction evaluation for real-life colour target.

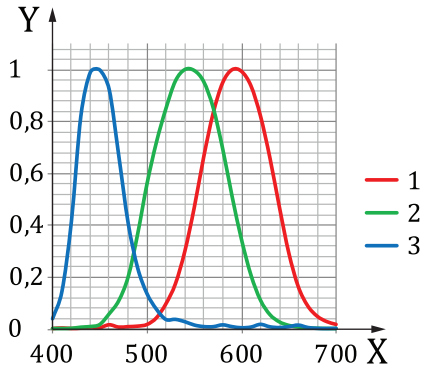

a) Normalized spectral distribution of OSSS A

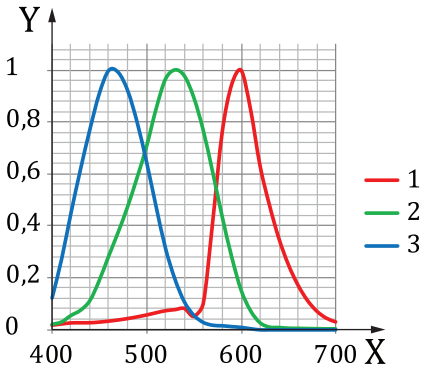

b) Normalized spectral distribution of OSSS B

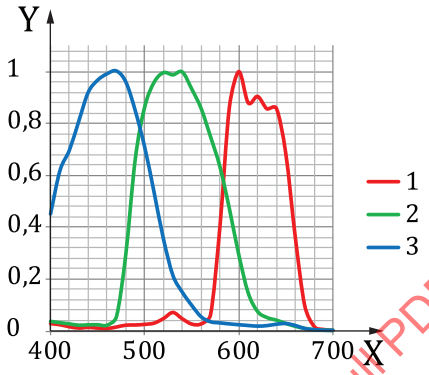

c) Normalized spectral distribution of OSSS C

Key

X wavelength, λ, in nm

Y relative sensitivity

Figure 5 — Normalized spectral distribution used in FOM calculations

Annex A
(informative)

Selection and eigenvectors of spectral distribution set

A.1 Selection of spectral distribution set

A wavelength range of 380 nm to 780 nm and a wavelength increment of 5 nm is illustrated here as an example suitable for wide-gamut applications. Each spectrum is therefore sampled at 81 wavelengths and the set of 81 principle components is calculated. The goal is to select a small set of these principle components with suitable weights such that the resulting spectral distribution set has many saturated colours. US Patent 5609978 described 190 colours. Many of the 190 colours were simply measured from Munsell, Pantone and other readily available colours sets. This data set was applied to colour calibration for three layers colour film. The data set chosen here has 190 colours of which 95 are saturated colours, 11 are achromatic colours, 5 have reflectance greater than 1 and 79 are mid-saturation colours. The eigenvectors are applied to the 95 saturated colours.

Spectral distribution data of the 95 saturated colours are described in Annex H.

NOTE US Patent 5609978 was already expired.

A.2 Eigenvectors of selected spectral distribution set

Figure A.1 shows the first eight most significant eigenvectors based on the 95 saturated colours. Table A.1 shows the first 8 eigenvectors and individual and cumulative contributions to total variance.

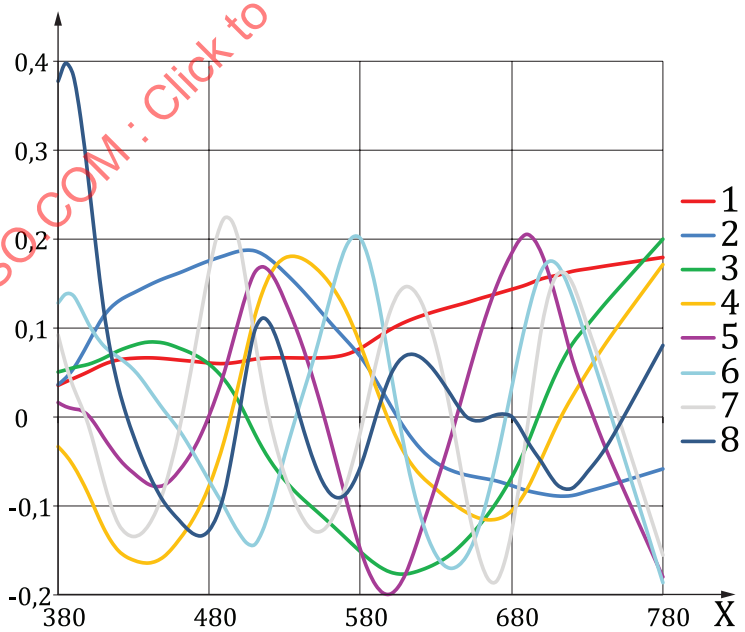

Key

X wavelength, λ, in nm

Figure A.1 — Eight most significant eigenvectors of 95 saturated colours

Table A.1 — First eight eigenvectors and individual contributions and cumulative contributions to the total variance of 95 saturated colours

	Eigenvalue	Individual contributions to the total variance	Cumulative contributions to the total variance
1st	2,760441	0,584623	0,584623
2nd	0,953441	0,201926	0,786549
3rd	0,558827	0,118352	0,904901
4th	0,283538	0,060049	0,964950
5th	0,071483	0,015139	0,980089
6th	0,032472	0,006877	0,986966
7th	0,022799	0,004828	0,991975
8th	0,018024	0,003817	0,995612

Annex B
(informative)

Colour gamut of boundary colour

A chroma value of boundary colour is dependent on the number of eigenvectors to be used. Figure B.1 shows the relationship between an average C^* and number of the eigenvectors to be used. Here, an average C^* is an average of maximum C^* value for each hue angle of boundary colours. The average C^* value is monotonically increasing with the number of the eigenvectors to be used. In this example, eight (N = 8) eigenvectors are selected as an appropriate number.

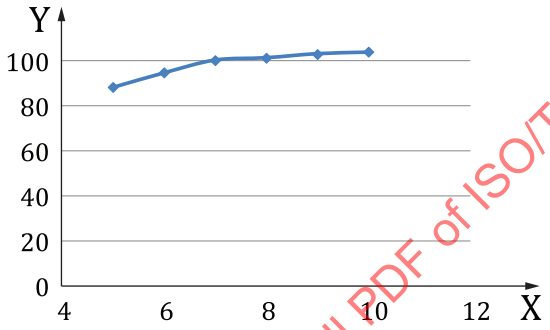

Key

X number of eigenvector

Y average C^*

Figure B.1 — Average C^* plot of boundary colours in case of eight eigenvector

Mathematical software packages provide very useful functions to calculate boundary colours using Formula (1). Weight w_j is determined to refer j-th eigenvector.

Figure B.2 shows CIE a^* -CIE b^* plot of boundary colours for eight eigenvectors. Boundary colours are calculated under illuminant E. Spectral distribution data of boundary colours for eight eigenvectors with 5° steps in hue angle are described in Annex H.

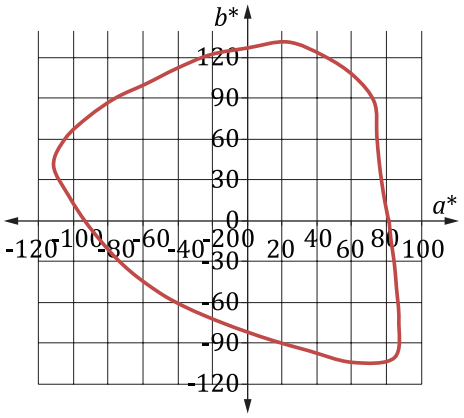

Figure B.2 — a^*-b^* plot of boundary colours in case of eight eigenvectors

Annex C
(informative)

Worked example for spectral distribution generation of Pointer's surface colours

C.1 General

The procedure of generation method of spectral distribution of highly-saturated colour targets corresponding to CIELAB values of Pointer's surface colours[6] based on the eigenvectors is described in the following paragraph. Detailed procedures are written as example method for readers convenience.

a) Calculation of objective colour chroma and $\frac{C^*_c}{C^*_r}$ ratio (See C.2)

b) Calculation of maximum $\frac{C^*_c}{C^*_r}$ ratio (See C.3)

c) Generation of spectral distribution candidates (See C.4)

NOTE A $\frac{C^*_c}{C^*_r}$ is a ratio of CIELAB C^* of calculated spectral distribution and CIELAB C^* of reference spectral distribution.

There are two steps for the optimization process (b) and c) above). The first step is described in C.2 and the purpose of this step is to obtain the relationship between $\frac{C^*_c}{C^*_r}$ and the number of required eigenvectors. The results of this first step is applied to obtain the colour gamut of the eigenvectors set and to determine the number of eigenvectors to be used in the second step. The second step is described in C.4 and the purpose of this step is to obtain the candidate spectral distribution for the highly-saturated spectra.

C.2 Calculation of objective colour chroma and $\frac{C^*_c}{C^*_r}$ ratio

Given any set of reference target colours (C^*_r), the 'objective colour' is the projection of the reference target colour onto the gamut of Pointer surface colours. The chromaticity of this colour is C^*_c and the calculation of the ratio $\frac{C^*_c}{C^*_r}$ is described as follows.

An objective colour chroma of reference colour target is set to Pointer's surface colour. Pointer's surface colour is described under illuminant *C*.

The reason why the objective colour chroma of Pointer's surface colour is selected is described in C.5. An objective colour chromaticity is determined as follows.

Suppose the colour of a reference colour target has L^* = 55,60, a^* = 41,44, b^* = 45,30, C^* = 61,40 and hue angle 47,55° and noting that the four corresponding CIELAB values of Pointer's gamut grid are:

A. L^* = 55,00, a^* = 71,24, b^* = 59,78, (C^* = 93,00, hue angle of 40,00°)

B. L^* = 55,00, a^* = 64,28, b^* = 76,60, (C^* = 100,00, hue angle of 50,00°)

C. L^* = 60,00, a^* = 67,41, b^* = 56,57, (C^* = 88,00, hue angle of 40,00°)

D. L^* = 60,00, a^* = 65,56, b^* = 78,14, (C^* = 102,00, hue angle of 50,00°)

Figure C.1 shows how to determine objective chromaticity using reference chromaticity and the four Pointer's surface colours as follows.

— Point C1 is found from the intersection of the straight line passing achromatic colour having CIELAB values (L^* = 55,00, a^* = 0,00, b^* = 0,00) with hue angle 47,55° and the straight line connecting A (L^* = 55,00, a^* = 71,24, b^* = 59,78) and B (L^* = 55,00, a^* = 64,28, b^* = 76,60).

— Point C2 is found from the intersection of straight line passing achromatic colour having CIELAB values (L^* = 60,00, a^* = 0,00, b^* =0,00) with hue angle 47,55° and the straight line connecting (L^* = 60,00, a^* = 67,41, b^* = 56,57) and (L^* = 60,00, a^* = 65,56, b^* = 78,14).

— The CIELAB values of C1 and C2 are (L^* = 55,00, a^* = 65,99, b^* = 72,48) and (L^*=60,00, a^*=66,02, b^*=72,85) respectively

— C_p is an interior division point and is calculated using three L^* points such as L^* = 55,00, L^* = 60,00 and L^* = 55,60. CIELAB values of C_p^* are (L^* = 55,60, a^* = 65,99, b^* = 72,53).

— The $\frac{C_p^*}{C_r^*}$ ratio is the ratio of C^* of Pointer's surface (C_p^*) and C^* of reference colour (C^*_r) ($\frac{C_p^*}{C_r^*}$ = 1,5971).

This is C*p/C*r ratio is used in C.4 as objective C* ratio.

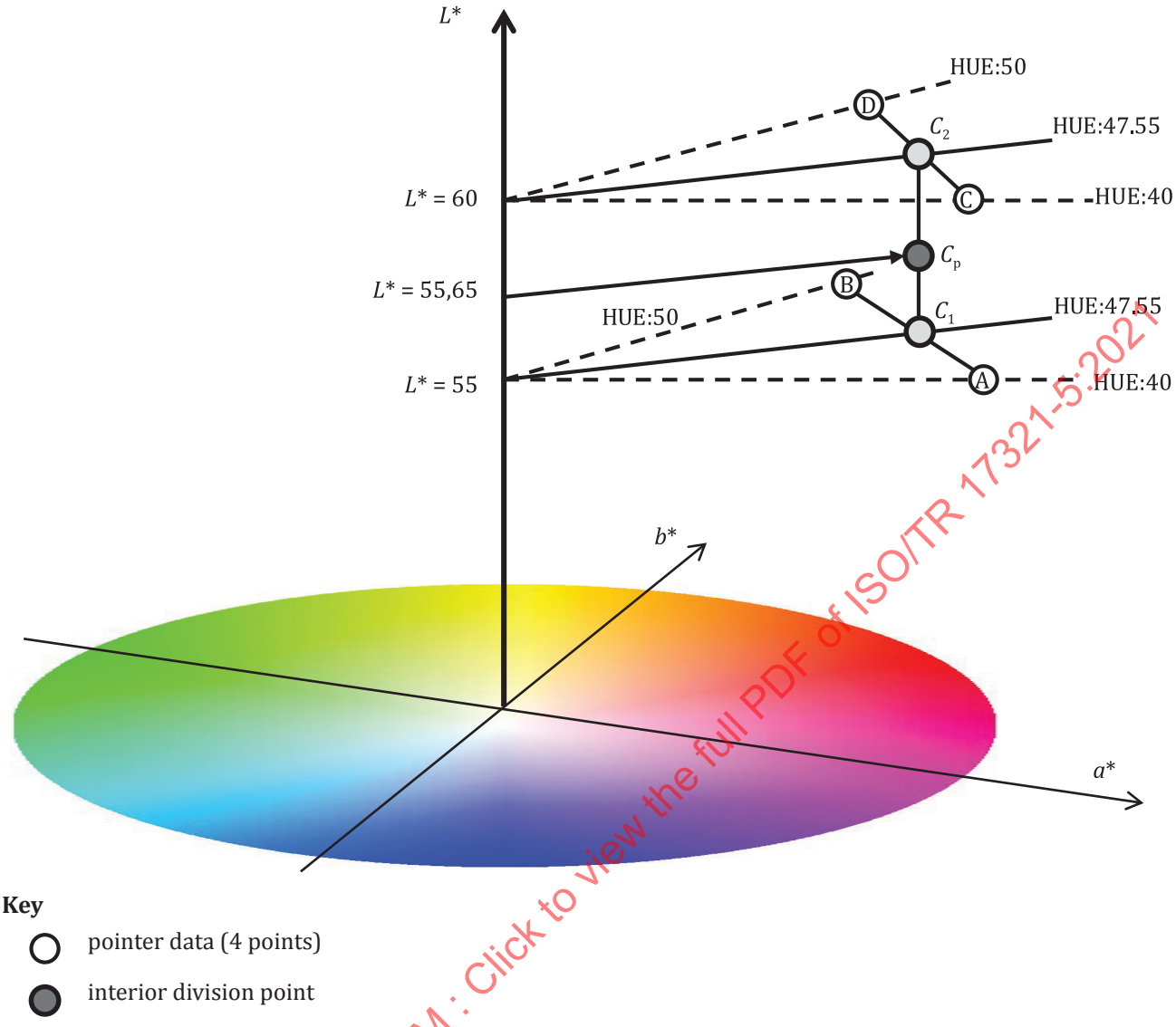

Key

- pointer data (4 points)
- interior division point

Figure C.1 — Calculation method of objective chromaticity of reference target

C.3 Calculation of maximum $\frac{C_c^*}{C_r^*}$ ratio

A $\frac{C_c^*}{C_r^*}$ ratio is a ratio of CIELAB C^* for the objective colour (whose spectral distribution is calculated using nonlinear numerical optimization) and CIELAB C^* of reference spectral distribution. This $\frac{C_c^*}{C_r^*}$ ratio is calculated for each reference target colour and the number of eigenvector to be used.

This $\frac{C_c^*}{C_r^*}$ ratio is optimized using nonlinear numerical optimization. Optimization details are as follows.

Notation:

— C_c^* : CIELAB C^* of calculated-spectral distribution using nonlinear numerical optimization;

— C_r^* : CIELAB C^* of spectral distribution of reference colour.

Input data:

— eigenvectors for 95 colours data set;

— chromaticity of a reference spectral distribution (CIELAB $L^*a^*b^*$ hue angle under illuminant C);

— weights of eigenvectors to reproduce reference spectral distribution (these are used as initial values for nonlinear numerical optimization).

Constraint conditions:

— $|\Delta L^*| < 0{,}5$;

— $|\Delta h| < 0{,}0001$ radians;

— spectral reflectance values constrained to the range [0,0,1,0].

Tuning parameters: intensities of eigenvectors

Objective metric: C_c^* of generated spectral distribution;

Optimization: maximization of $\frac{C_c^*}{C_r^*}$ for each reference target colour and number of eigenvectors.

Output data:

— Maximum value of $\frac{C_c^*}{C_r^*}$ for each reference target colour and number of eigenvectors;

— Calculated spectral distribution candidate for highly-saturated colour target.

$\frac{C_c^*}{C_r^*}$ ratios of several colour target are shown in Table C.1. Maximum $\frac{C_c^*}{C_r^*}$ in Table C.1 is maximum value of $\frac{C_c^*}{C_r^*}$ values of 7, 9, 11, 13, 15, 17, 19 and 26 eigenvectors. These maximum values are described as red characters in Table C.1. Pointer's $\frac{C_c^*}{C_r^*}$ is calculated as described in C.2.

The maximum value of $\frac{C_c^*}{C_r^*}$ for number of vectors and each colour patch aim value is strongly dependent on the initial values of the eigenvectors. Consider CT-78 in Table C.1 where the maximum intensity value $\frac{C_c^*}{C_r^*}$ is obtained for 11 eigenvectors, the other intensity values are set to zero and 11 eigenvectors optimization is performed. This relationship is applicable to all of other colour patch aim values.

Table C.1 — $\frac{C^*_c}{C^*_r}$ ratio

Colour target number	7-V $\frac{C^*_c}{C^*_r}$	9-V $\frac{C^*_c}{C^*_r}$	11-V $\frac{C^*_c}{C^*_r}$	13-V $\frac{C^*_c}{C^*_r}$	15-V $\frac{C^*_c}{C^*_r}$	17-V $\frac{C^*_c}{C^*_r}$	19-V $\frac{C^*_c}{C^*_r}$	26-V $\frac{C^*_c}{C^*_r}$	Maximum $\frac{C^*_c}{C^*_r}$	Pointer's $\frac{C^*_c}{C^*_r}$
CT-24	1,092	1,143	1,186	1,181	1,154	1,113	1,188	1,085	1,188	0,947
CT-29	1,157	1,216	1,221	1,256	1,260	1,110	1,270	1,115	1,270	1,166
CT-44	1,451	1,565	1,514	1,624	1,276	1,484	1,352	1,315	1,624	1,657
CT-64	1,269	1,269	1,251	1,259	1,243	1,249	1,256	1,248	1,269	1,010
CT-78	1,261	1,241	1,447	1,437	1,371	1,316	1,371	1,237	1,447	1,115
CT-93	1,213	1,129	1,170	1,256	1,251	1,186	1,197	1,103	1,256	0,913
CT-111	1,556	1,816	1,783	1,982	1,798	1,488	1,593	1,311	1,982	1,351
CT-133	1,078	1,087	1,174	1,124	1,079	1,075	1,066	1,109	1,174	1,174
CT-146	1,492	1,571	1,529	1,309	1,266	1,290	1,319	1,208	1,571	1,254
CT-174	2,178	2,341	2,351	2,405	2,300	2,463	2,320	2,128	2,463	1,489

There are three cases for C^*_p, C^*_c and C^*_r.

a) $\frac{C^*_p}{C^*_r}$ ratio < 1,0 (reference has higher chroma than corresponding Pointer surface colour)

This case includes CT-24 and CT-93 in Table C.1. It is possible to generate spectral distribution having $\frac{C^*_p}{C^*_r}$ ratio.

b) Maximum $\frac{C^*_c}{C^*_r} > \frac{C^*_p}{C^*_r}$ (candidate colour has higher chroma than Pointer surface colour)

This case includes CT-29, CT-64, CT-78, CT-111, CT-146 and CT-174 in Table C.1. It is possible to generate spectral distribution having C^*_p/C^*_r ratio. Most of 95 colour targets are case b).

c) Maximum $\frac{C^*_c}{C^*_r} < \frac{C^*_p}{C^*_r}$ (candidate colour has lower chroma than Pointer surface colour)

This case includes CT-44 and CT-133 in Table C.1. It is impossible to generate spectral distribution having $\frac{C^*_p}{C^*_r}$ ratio. Then $\frac{C^*_c}{C^*_r}$ of generated-spectral distribution candidate become smaller than $\frac{C^*_p}{C^*_r}$.

NOTE Colour target number such as CT-93 is number of 190 colour target set described in Annex H.

NOTE Hue angle constraint condition is very important. Shape of calculated-spectral distribution is very dependent on Hue angle constraint condition. Then very tight constraint condition for hue angle is determined as 0,0007 radian.

C.4 Generation of spectral distribution candidates

It is possible to calculate the maximum C^* chromaticity for each reference target using the maximum $\frac{C^*_c}{C^*_r}$ in Table C.1 and calculate the colour gamut achievable by the eigenvectors set. The Reference target colour in this calculation consists of 95 colour target set described in 4.2.2. Figure C.2 shows three gamut boundaries (Pointer's surface colour, the eigenvectors set and Munsell colour system) for three L* levels under illuminant C. Objective colour gamut of calculated highly-saturated spectral distribution

is selected as Pointer's surface colour because Pointer's surface colour gamut is larger than real targets of Munsell colour system.

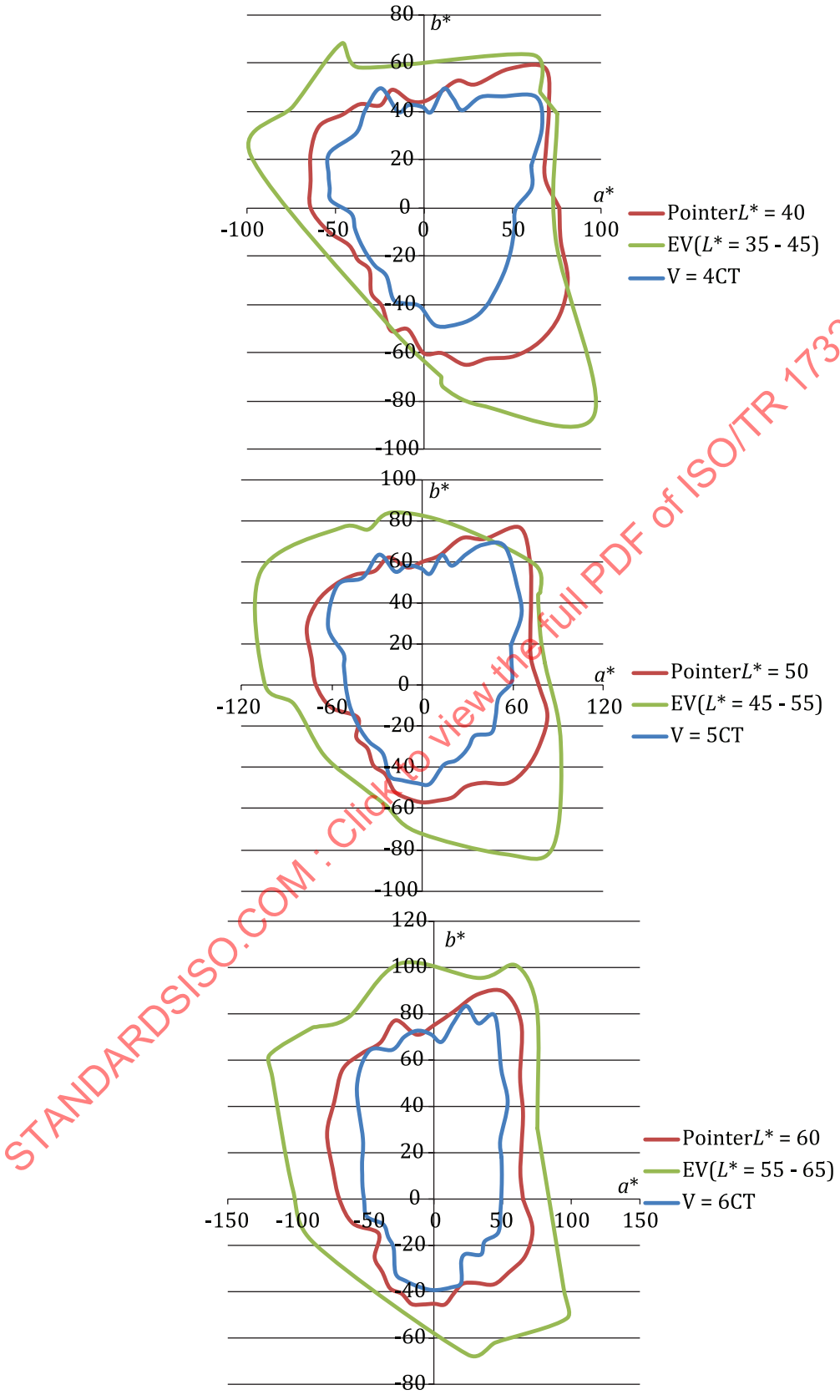

Figure C.2 — Three *a-*b** diagrams of reproducible distribution spectrum of the eigenvectors and Pointer's surface colours and real targets of Munsell colour system for three *L** levels**

At first, appropriate numbers of eigenvectors for each reference target are selected using Table C.1. Several examples are described below:

Reference target number 78 : 11, 12 and 13

Reference target number 93 : 11, 13 and 15

Reference target number 133 : 10, 11 and 12

Reference target number 146 : 9, 11 and 13

NOTE Large number of eigenvector might make better shape of calculated-spectral distribution.

This $\frac{C_c^*}{C_r^*}$ ratio is optimized using nonlinear numerical.

Optimization details are as follows. Input data, constraint conditions and tuning parameters for this optimization are same as described in Annex C.3.

Additional notation :

— C_p^*: CIELAB C* of Pointer's surface corresponding to reference colour

Objective metric : $|C_c^* - C_p^*|$ of generated spectral distribution

Optimization : Minimization of $|C_c^* - C_p^*|$ for each reference colour target and several selected-number of eigenvectors.

Output data :

— Value of $|C_c^* - C_p^*|$

— Calculated spectral distribution candidate for highly-saturated colour target

Several calculated-spectral distribution candidates for each reference target are generated using appropriate number of eigenvectors.

NOTE Hue angle constraint condition is very important. Shape of calculated-spectral distribution is very dependent on Hue angle constraint condition. Then very tight constraint condition for hue angle is determined as 0,0007 radian.

There are some recommendations for evaluation to select calculated-spectral distribution candidates.

First criterion is that the value of $|C_c^* - C_p^*|$ is within 1,00.

Second criterion is the shape of the spectral distribution. There is one method to determine. This criterion is a visual check. Criteria for this visual check are that the spectrum has no side lobe and needs to be smooth and realistic.

Figure C.3 shows candidate-spectral distributions of three colours described in Annex C.3. The term n-V in Figure C.3 means 'n- eigenvectors', so 11-V means that 11 eigenvectors are used. Table C.2 shows $\frac{C_c^*}{C_r^*}$ and $\frac{C_p^*}{C_r^*}$ values for four colours. Spectral distributions with 11-V of CT-78, with 11-V of CT-93, with 12-V of CT-133, and with 13-V of CT-146 are selected for highly-saturated spectral distributions respectively.

Highly-saturated spectral distributions of 95 colour targets are described in Annex H.

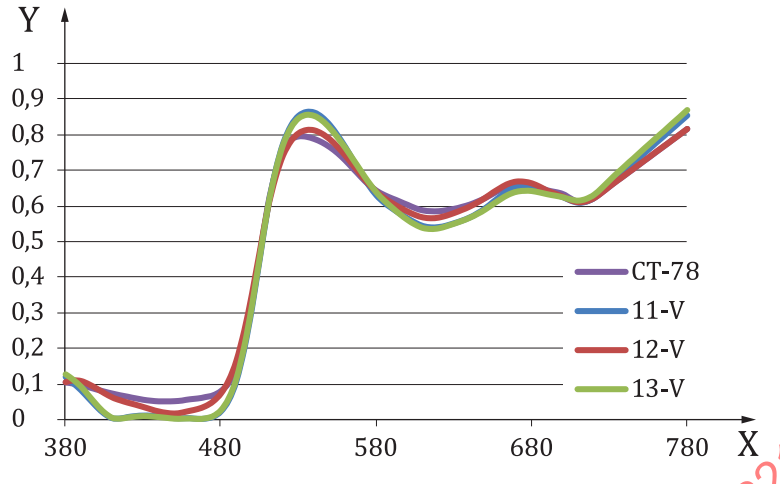

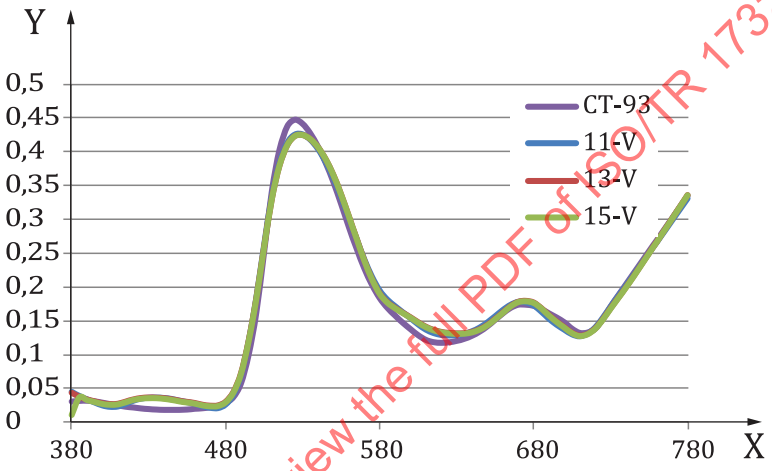

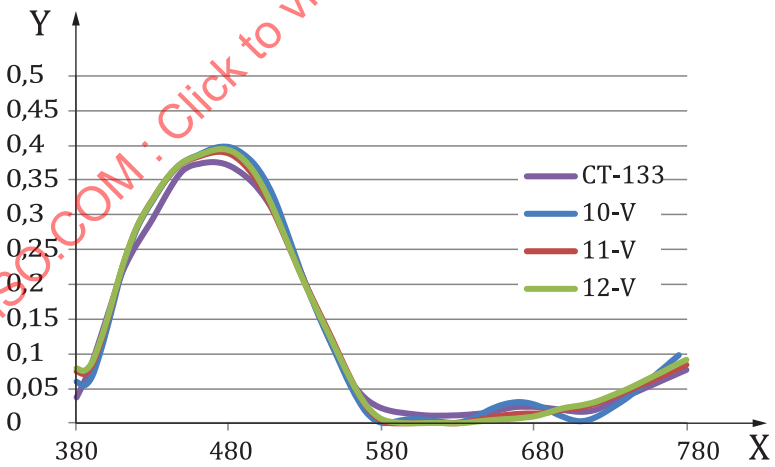

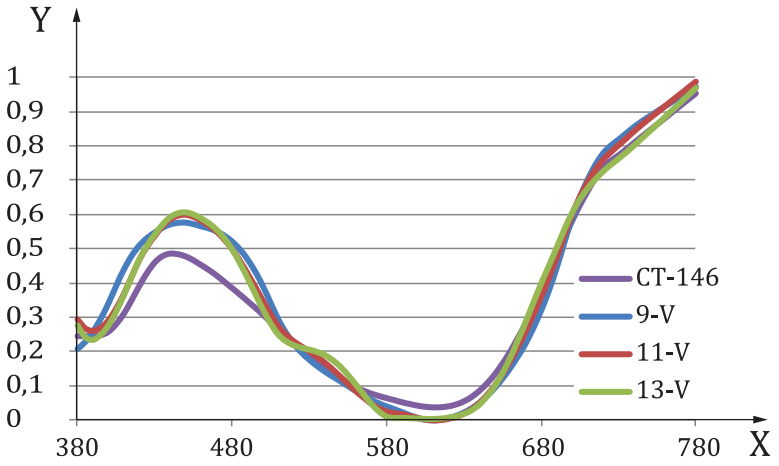

Key

X wavelength, λ, in nm

Y reflectance

Figure C.3 — Candidated-spectral distributions of four colour targets

Table C.2 — $\frac{C_c^*}{C_r^*}$ and $\frac{C_p^*}{C_r^*}$ values for four colour targets

Colour target , n-V	$\frac{C_c^*}{C_r^*}$	$\frac{C_p^*}{C_r^*}$
CT-78		
11-V	1,1154	1,2777
12-V	1,1154	1,1154
13-V	1,1154	1,2777
CT-93		
12-V	0,9130	0,9130
13-V	0,9130	0,9130
14-V	0,9130	0,9130
CT-133		
19-V	1,1745	1,0845
20-V	1,1745	1,0750
21-V	1,1745	1,0788
CT-146		
31-V	1,1154	1,1154
61-V	1,1154	1,1154
81-V	1,1154	1,1154

Annex D
(informative)

Background information for defining CDSW

This Annex is described the necessity to define the formula *Fac_a** and *Fac_b** .

First, to understand how to define CDSW, the colour differences of Cameras ($\mu \approx 1$) at each wavelength were investigated. Camera A and camera B are selected as examples of colorimetric cameras ($\mu \approx 1$). Their spectral sensitivities were measured and used to define a conversion matrix from sensor RGB to XYZ tristimulus values. The optimization to obtain conversion matrix from camera sensitivity to colour matching function was carried out using the least squares method. The transformed spectral sensitivities of the two cameras are shown in Figure D.1 overlapped with colour matching function.

The transformed spectral sensitivities of the two cameras are shown in Figure D.1 overlapped with colour matching function.

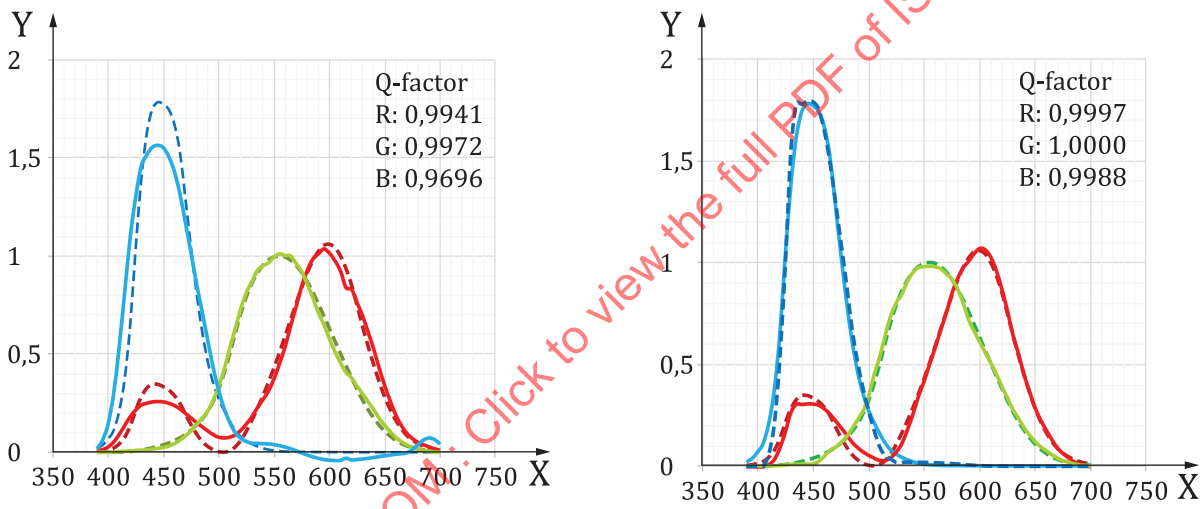

Key

X wavelength, λ, in nm

Y relative sensitivity

Figure D.1 — (Left). Spectral sensitivity of Camera A (solid curve) and CMF (dotted curve). (Right). Spectral sensitivity of Camera B (solid curve) and CMF (dotted curve).

The colour difference (ΔE_{00}) between colour matching function and spectral sensitivity of Camera A and Camera B was calculated for very narrow band spectra of every wavelength and these colour differences are shown in Figure D.2. The main components of the colour difference, ΔL^*, $\Delta a^*$and Δb^* are plotted against wavelength in Figure D.3 for further investigation. The ΔL^*, $\Delta a^*$and Δb^* are defined by Formulae (D.1), (D.2) and (D.3).

NOTE The ΔE_{00} is specified in ISO/CIE 11664-6:2014.

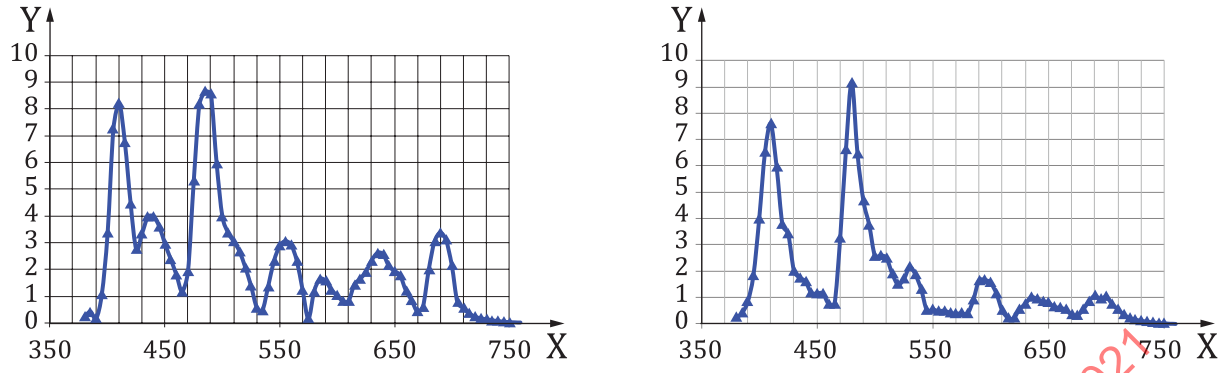

Key

X wavelength, λ, in nm

Y colour difference, ΔE_{00}

Figure D.2 — Colour differences of camera A (left) and camera B (right)

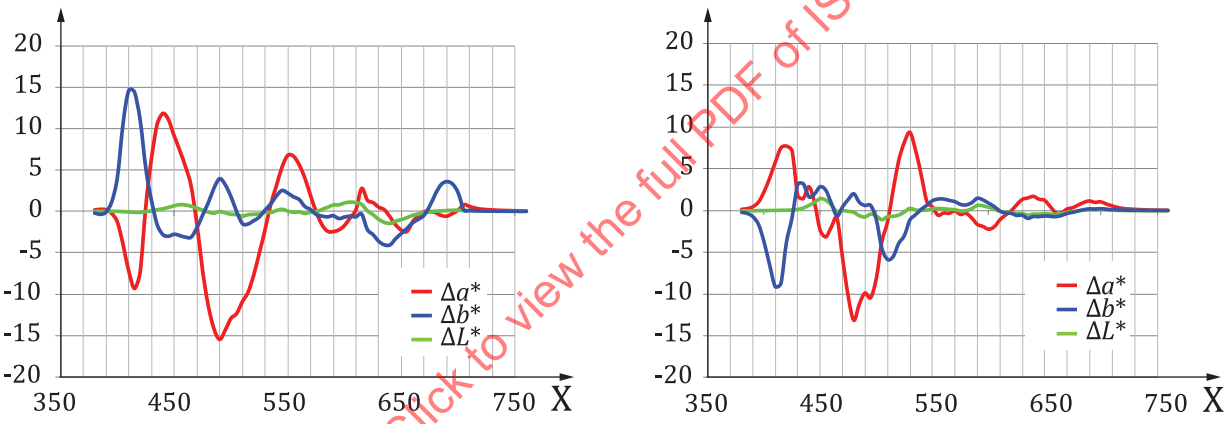

Key

X wavelength, λ, in nm

Figure D.3 — Main components of colour difference on camera A (left) and camera B (right)

Comparing these figures shows that colour difference is largely dependent on the wavelength and has a mountain shaped distribution. The peak wavelengths of colour difference are similar to those of the absolute values of main components, Δa^* and Δb^*. ΔL^* has little effect on the colour difference over all wavelengths. This means that Y is the same between the colour matching functions and the transformed spectral sensitivities of camera A and camera B. For this reason, ΔL^* can be set to zero for the remainder of this analysis as shown in Formulae (D.4) and (D.5). The values of Δa^* and Δb^* are dominated by X and Z, respectively.

$$\Delta L^* = 116 \times \left\{ f\left(Y_{caX} / Y_n \right) - f\left(Y_{CMF} / Y_n \right) \right\} \tag{D.1}$$

$$\Delta a^* = 500 \times \left\{ f\left(X_{caX} / X_n \right) - f\left(Y_{caX} / Y_n \right) \right\} - 500 \times \left\{ f\left(X_{CMF} / X_n \right) - f\left(Y_{CMF} / Y_n \right) \right\} \tag{D.2}$$

$$\Delta b^* = 200 \times \left\{ f\left(Y_{caX} / Y_n \right) - f\left(Z_{caX} / Z_n \right) \right\} - 200 \times \left\{ f\left(Y_{CMF} / Y_n \right) - f\left(Z_{CMF} / Z_n \right) \right\} \tag{D.3}$$